Geochemical Perspectives Letters

High δ^{26}Mg in an early Cambrian palaeosol reveals a terrestrial clay mineral factory

Z.-H. Huang, N.M. Rabideaux, S.C. Peters

Supplementary Information

The Supplementary Information includes:

- Samples and Methods
- Tables S-1 to S-3
- Figures S-1 to S-3
- Supplementary Information References

Samples and Methods

Sample location and description.
The bulk geochemistry of the Wind River Canyon palaeosol (43°27'51'' N, 108°10'14'' W) was previously described by Z. Huang *et al*. (2024) and its geologic location is marked in **Figure S-1**. A total of 11 bulk samples, including 10 saprolites and 1 unweathered bedrock, were selected for this study. The saprolite samples show consistent TiO_2/Al_2O_3 ratios throughout the profile, indicating that the palaeosol was developed in situ on the bedrock.

Pre-digestion sample processing.
Bulk geologic samples from the palaeo-weathering profile were first reduced to chips and then rinsed with Milli-Q grade water several times to minimize contamination from dust during the cutting process. The chips were then crushed with a jaw crusher or a rock hammer. Crushed samples were then pulverized for approximately 10 mins in a Tungsten Carbide ball mill for bulk geochemical, mineralogical, and isotopic analyses.

The clay fraction ($r < \sim 2\mu m$) of 7 saprolite samples was further separated from the crushed bulk samples for elemental and isotopic analyses. At least 5 to 10 g of saprolite samples or their chips were gently crushed using an agate mortar and pestle and then suspended in Milli-Q double de-ionized water (Ω = 18.2 M). The suspensions were then shaken and vortexed repeatedly. Suspended samples are then settled over a required period according to Stokes' law (assuming room temperature at 25 °C). The supernatant containing clay-sized suspensions was then decanted and collected. The clay suspensions are shaken and divided into 2 aliquots for geochemical and Mg isotopic analyses. Flakes of dried clay extracts were then collected from acid-cleaned Teflon beakers after evaporation on a hotplate at ~75 to 95 °C.

Sample digestion and column chemistry.

For the major elemental analyses, the bulk rock powder and the clay fraction of each saprolite sample were digested using a conc. trace metal grade HF and house distilled HNO_3 mixture in acid-cleaned 7 mL Savillex Teflon beakers on a hotplate at 90 to 100 °C for at least 72 hrs to achieve complete dissolution. Solutions were dried overnight and refluxed with a mixture of ~6 N house distilled HCl and conc. HNO_3 for approximately 24 hrs to eliminate fluorides and then dried down at 80 °C. After complete digestions, all samples were re-dissolved and diluted in ~1 N house distilled HNO_3. Major elements of bulk samples and clay-sized fractions were measured by quadrupole ICP-MS (Thermal Elemental X-series, Winsford, UK) at the Earth and Environmental Sciences Department of Lehigh University.

For Mg isotopic analyses, bulk rock-powder samples (~200 mg) or clay extracts were weighed into 5 mL Teflon beakers. Then 2 mL of conc. HF and 0.5 mL of HNO_3 were added. Samples were left on a hot plate for 48 h with lids on before evaporation to dryness. The samples were repeatedly refluxed in aqua regia to minimize fluorides and evaporated to dryness. Mg was separated from matrix elements with a 3-step column chemistry through AG 50W X-8 (200 to 400 mesh) and AG MP-1M (100 to 200 mesh) ion exchange resins. The detailed steps are listed in **Table S-1** and are modified from Huang *et al*. (2009) and Wombacher *et al*. (2009). The preparation blank contribution is below 0.1 % of Mg content in samples. The measurements are carried at ALS Scandinavia, Luleå, Sweden by MC-ICP-MS (NEPTUNE PLUS, ThermoScientific) using internal standardization and external calibration with bracketing isotope SRMs. Delta values for Mg were reported against the DSM-3 and were calculated as following (Young and Galy, 2004):

$$\delta^{X}Mg = [(^{X}Mg/^{24}Mg)_{sample} / (^{X}Mg/^{24}Mg)_{DSM\text{-}3} - 1] * 1000, \text{ with } X = 25 \text{ or } 26 \quad (1)$$

Geological reference materials, including IRMM-3704 and JB-2, were also measured to ensure the reproducibility and accuracy of the measurements. A three-isotope plot with $\delta^{25}Mg$ vs $\delta^{26}Mg$ (DSM3, ‰) (**Fig. S-2**) shows all analytical results follow a mass-depended fractionation.

Bulk quantitative X-ray Diffraction (QXRD).

Bulk powder XRD analysis was completed on a Rigaku MiniFlex 6G in the Chemistry Department at Rutgers University-Newark. Samples were measured from 5° to 70° 2θ at 40 kV and 15 mA with a 0.01° step size at a rate of 2°/min. Phase identification was completed using Rigaku's Smart Lab Studio Plus II software package with reference to the Crystallographic Open Database (COD), Moore and Reynolds (1997), and Brindley and Brown (1980). The reference intensity ratio (RIR) method was applied for quantitative XRD analyses. The RIR method scales all diffraction data to a standard, most commonly corundum, with a scale factor defined as:

$$\text{Intensity Analyte/Intensity Corundum} = I/Ic \quad (2)$$

The COD includes the I/Ic for most mineral reference patterns, and only reference patterns with I/Ic values were used in these analyses. Diffraction peaks are matched with corresponding mineral phases, producing a quantitative abundance for each assigned phase. Detailed bulk quantitative XRD reports were generated for each sample.

Supplementary Tables

Table S-1 Mg Column chemistry purification procedure. Note that the last step was repeated for 2 times if necessary for complete separation of Mg from Al.

Table S-2 Elemental, Clay mineralogical, and Mg isotopic compositions of 11 bulk samples from the weathering profile, 7 clay fraction samples, duplicates, and geological reference materials. CIA and PIA values for bulk samples are from Huang *et al*. (2024).

Table S-3 Chemical Index of Alteration values and δ^{26}Mg of reported modern felsic saprolite and soil samples from literature and the early Cambrian palaeosol from this study.

Tables S-1 to S-3 are available for download (.xlsx) from the online version of this article at http://doi.org/10.7185/geochemlet.2521.

Supplementary Figures

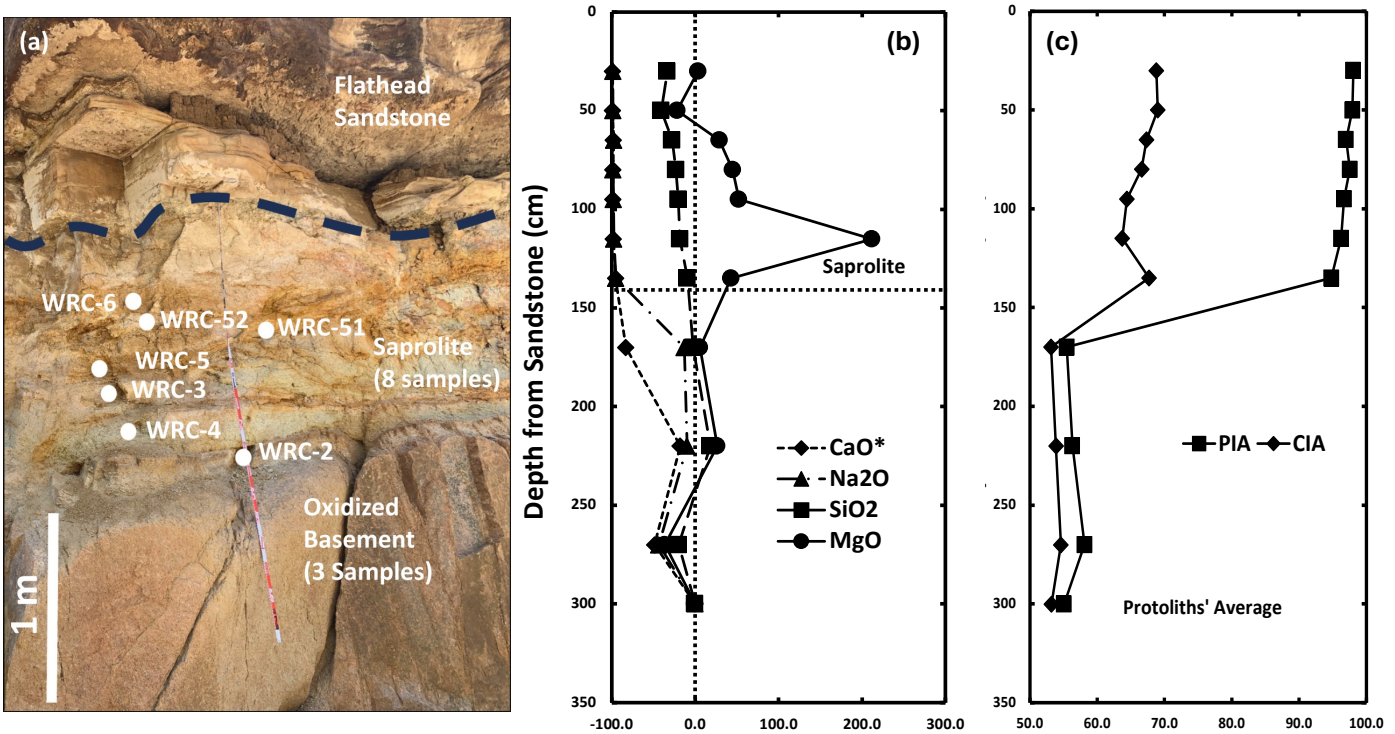

Figure S-1 The saprolite zonation showing the geochemical and isotopic composition of the palaeosol profile: **(a)** The outcrop showing the Wind River Canyon palaeo-weathering profile and approximate sampling locations; **(b)** the mass-balance calculation (Zr as the immobile element) showing the loss and addition of major elements of the saprolite; and **(c)** the vertical variation of the CIA (Chemical Index of Alteration) and PIA (Plagioclase Index of Alteration) across the weathering profile.

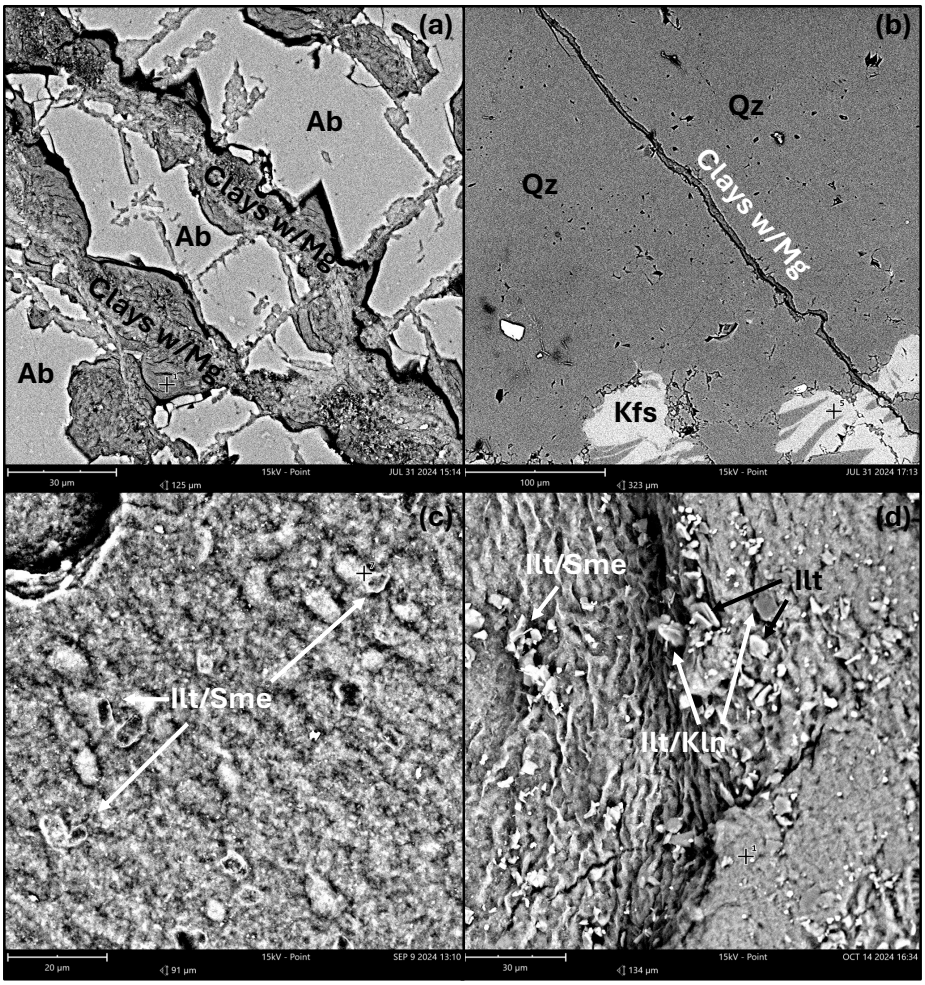

Figure S-2 The weathering features and clay mineralogy of the saprock samples and clay-sized portion of the saprolite samples observed under the SEM-BSE. The thin section of saprock samples **(a, b)** shows the filling of cracks with Mg-containing clay minerals between primary minerals such as quartz and albite grains. The clay-sized fractions extracted from two saprolite samples show an assemblage of smectite, kaolinite, and illite in the lower saprolite **(c)**, and illitized smectite and kaolinite in the upper saprolite **(d)**.

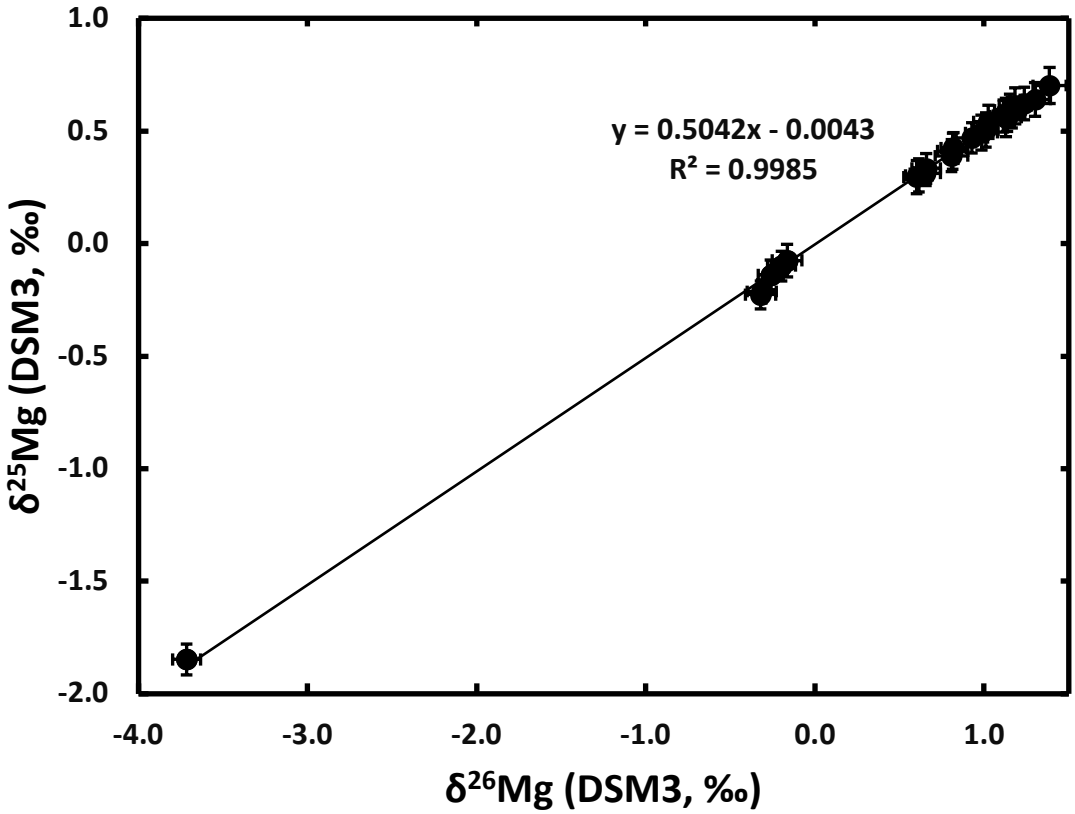

Figure S-3 The three-isotope plot with δ^{25}Mg *vs.* δ^{26}Mg (DSM3, ‰) for all samples and standards analysed in this study. The analytical results for geologic standard JB-2 agree with previously published data (Teng, 2017). The linear trendline follows a mass-dependent fractionation with a slope of 0.5042.

Supplementary Information References

Brewer, A., Teng, F.Z., Dethier, D. (2018) Magnesium isotope fractionation during granite weathering. *Chemical Geology* 501, 95–103. https://doi.org/10.1016/j.chemgeo.2018.10.013

Brindley, G.W., Brown, G. (1980) *Crystal Structures of Clay Minerals and their X-ray Identification*. Mineralogical Society of Great Britain and Ireland, London. https://doi.org/10.1180/mono-5

Fan, B.L., Yang, X.Q., Jiang, K., Zhao, Z.Q. (2023) Processes controlling the Mg isotope behavior during granite weathering. *Journal of Asian Earth Sciences* 251, 105674. https://doi.org/10.1016/j.jseaes.2023.105674

Gao, T., Qi, M., Wang, Z., Yin, R., Liu, C., Liu, Y., Ke, S., Zhao, Z.-Q. (2023) Magnesium Isotope Variations in Granite Regoliths from Two Contrasting Climates. *Journal of Geophysical Research: Earth Surface* 128, e2023JF007217. https://doi.org/10.1029/2023JF007217

Huang, F., Glessner, J., Ianno, A., Lundstrom, C., Zhang, Z. (2009) Magnesium isotopic composition of igneous rock standards measured by MC-ICP-MS. *Chemical Geology* 268, 15–23. https://doi.org/10.1016/j.chemgeo.2009.07.003

Huang, Z., Peters, S.C., Pazzaglia, F.J., Hernandez, M. (2024) A chemical weathering and paleoclimatic reconstruction of the early Cambrian environment of the Wyoming Craton from the Wind River Canyon, WY paleosol on the Great Unconformity. *Precambrian Research* 409, 107447. https://doi.org/10.1016/j.precamres.2024.107447

Li, M.Y.H., Teng, F.-Z., Zhou, M.-F. (2021) Phyllosilicate controls on magnesium isotopic fractionation during weathering of granites: Implications for continental weathering and riverine system. *Earth and Planetary Science Letters* 553, 116613. https://doi.org/10.1016/j.epsl.2020.116613

Moore, D.M., Reynolds Jr., R.C. (1997) *X-ray Diffraction and the Identification and Analysis of Clay Minerals*. Oxford University Press, Oxford.

Teng, F.-Z. (2017) Magnesium Isotope Geochemistry. *Reviews in Mineralogy and Geochemistry* 82, 219–287. https://doi.org/10.2138/rmg.2017.82.7

Wombacher, F., Eisenhauer, A., Heuser, A., Weyer, S. (2009) Separation of Mg, Ca and Fe from geological reference materials for stable isotope ratio analyses by MC-ICP-MS and double-spike TIMS. *Journal of Analytical Atomic Spectrometry* 24, 627–636. https://doi.org/10.1039/B820154D

Young, E.D., Galy, A. (2004) The Isotope Geochemistry and Cosmochemistry of Magnesium. *Reviews in Mineralogy and Geochemistry* 55, 197–230. https://doi.org/10.2138/gsrmg.55.1.197